ISSN 2411-3336; e-ISSN 2541-9404

JOURNAL OF MINING INSTITUTE

Zapiski Gornogo instituta

Journal homepage: pmi.spmi.ru

Research article

Geotechnical Engineering and Engineering Geology

Influence of daily fluctuations in thermodynamic parameters of atmospheric air on its temperature distribution in downcast shafts of potash mines

Mikhail A. Semin, Evgenii V. Kolesov✉, Ruslan R. Gazizullin, Stanislav V. Maltsev

Mining Institute of the Ural Branch of the RAS, Perm, Russia

How to cite this article: Semin M.A., Kolesov E.V., Gazizullin R.R., Maltsev S.V. Influence of daily fluctuations in thermodynamic parameters of atmospheric air on its temperature distribution in downcast shafts of potash mines. Journal of Mining Institute. 2026. Vol. 277, p. 94-106.

Abstract

The amplitude of diurnal variations in atmospheric air temperature may exceed 25 °C depending on the climatic zone and season. This gives rise to unsteady heat-transfer processes in downcast mine shafts and in the subsequent underground workings along the airflow path. The present study focuses on investigating the damping effect of the amplitude of diurnal fluctuations in the thermodynamic parameters of atmospheric air in downcast shafts of potash mines. The thermal damping effect consists in the attenuation of air temperature fluctuation amplitude as the airflow moves down the shaft due to heat exchange with the shaft lining and mass-transfer processes. A combined theoretical and experimental approach is proposed to predict air microclimate parameters at the junction of a downcast shaft with an underground level using a conjugate convective-diffusive heat and mass transfer model that accounts for processes in the shaft air, the lining, and the surrounding rock mass. A methodology for conducting *in situ* measurements at the study sites is described, the necessary experimental and calculation parameters are provided, and field measurement data obtained for two downcast shafts of potash mines with different depths are presented. The experimental data were used to validate the proposed model. The agreement between measured and calculated results confirms the suitability of the selected model for predicting air temperature at the shaft-underground level junction. Effective heat-transfer coefficients between the airflow and the shaft wall were determined for both downcast shafts, along with effective thermal diffusivities of the surrounding rock mass. An empirical relationship was established for the air temperature in the shaft bottom chamber of the underground level as a function of the daily mean temperature, the amplitude of surface temperature fluctuations, and the shaft depth.

Keywords

mine ventilation; daily temperature fluctuations; thermal regime of mine workings; downcast shaft; modeling; thermal damping effect; coupled heat and mass transfer; heat-transfer coefficient; rock thermal diffusivity

Funding

The study was carried out with financial support from the Ministry of Science and Higher Education of the Russian Federation within the framework of the State assignment “Monitoring, modeling, and control of aerological and thermophysical processes in complex mining and technical systems”.

Received: 12.08.2024 ***Accepted: 09.12.2025*** ***Online: 11.02.2026*** ***Published: 27.02.2026***

Introduction

Atmospheric air entering a mine shaft is subject to both diurnal and seasonal temperature variations. Seasonal temperature fluctuations have been actively studied since the mid-20th century, particularly in relation to mines in northern regions operating under natural thermal regimes [1]. Seasonal temperature variations exert a substantial influence on the thermal conditions of underground workings, extending even to remote working areas [2-4]. Diurnal temperature variations, by contrast, affect the thermal regime of mine workings to a lesser extent [5]. Interest in this phenomenon has intensified only

This is an open access article under the CC BY 4.0 license

in recent decades, as advances in microclimate control technologies and in mathematical methods for evaluating their efficiency have reached a level at which accurate design of ventilation and air-conditioning systems [6-8] requires accounting for additional thermal factors of an unsteady nature [9-11].

The amplitude of diurnal atmospheric air temperature fluctuations depends on the climatic zone and the season of the year and may exceed 25 °C [12]. This leads to the development of unsteady heat-transfer processes in downcast shafts and in the subsequent mine workings along the airflow path [13]. A large portion of the temperature fluctuation amplitude is damped by the downcast shafts themselves [14]. According to some studies [15], the amplitude of temperature oscillations at the junction of a downcast shaft with underground levels is relatively small. However, other investigations [12, 16] indicate that this amplitude can be significant and, in some cases, exceed 10 °C. As correctly noted in [17], the intensity of this phenomenon depends on shaft parameters. That study also identifies the main parameters influencing air-temperature variation at the junction of downcast shafts with the shaft bottom workings (Table 1). In our view, this classification is incomplete, since the listed factors are in many cases interrelated or mutually dependent.

Table 1

Main factors determining the influence of daily temperature variation at the underground level [17]

Atmospheric factors	Physical factors	Dynamic factors
Atmospheric air temperature	Shaft diameter	Airflow rate
Atmospheric relative humidity	Shaft shape	Air travel time
Barometric pressure	Shaft wall roughness	Contact time with surfaces
Presence of water inflows in the shaft	Shaft wall moisture	
Air density	Shaft equipment	

It should be emphasized that, with increasing production capacities, mines require progressively larger volumes of fresh air [18]. This challenge becomes even more pronounced when developing deep-lying levels [19-21]. As a result, both the characteristic dimensions of designed shafts and the ratio of shaft cross-sectional area to its perimeter increase, which reduces the influence of heat exchange with the shaft walls [22, 23] and enhances the thermal damping effect [24, 25]. For this reason, the phenomenon in question requires further investigation.

From a practical standpoint, the study of thermal damping is important for several reasons. First, accurate prediction of dry- and wet-bulb temperatures at the junction of a downcast shaft with an underground level is critical for assessing microclimatic conditions in mine ventilation networks and for deciding whether air-cooling systems are required to ensure acceptable working conditions in mines [26-28]. Second, it is essential for calculating natural ventilation pressure under both normal and reversed ventilation modes, since diurnal temperature variations can produce daily fluctuations in natural draft exceeding 500 Pa for shafts with depths of about 1 km. Third, it is necessary to improve the accuracy of emergency ventilation calculations in mines [29]. As is well known, air distribution in reversed ventilation modes changes, among other reasons, due to variations in natural draft. When the direction of airflow reverses, air temperature in the shafts changes, leading to the development of unsteady heat-transfer processes [11].

The first *in situ* measurements confirming the smoothing of temperature fluctuation amplitudes in downcast shafts were reported in [16]. The concept of the thermal damping effect was introduced, and it was hypothesized that its influence on the thermal regime of shaft bottom workings would differ for different shafts [26]. Analytical solutions accounting for the effect of thermal damping based on unsteady heat and mass transfer processes were subsequently developed and have been implemented in mine ventilation simulators. Experimental observations of the thermal damping effect in polymetallic mines in Canada were also reported, demonstrating that the phase of periodic air-

This is an open access article under the CC BY 4.0 license

temperature variations changes between summer and winter. In study [30], continuous temperature monitoring data collected over one week at various locations of a gold-copper mine were obtained and analyzed to identify and quantitatively assess the behavior of the thermal flywheel effect. That study showed that this phenomenon cannot be adequately described using steady-state thermal models.

In studies [12, 17], the theoretical interpretation of measurements of diurnal temperature variation in downcast shafts was carried out using neural-network approaches. In particular, a NARX neural-network algorithm was employed in [12, 17] to predict air temperature in shaft bottom workings. In [31, 32], a model based on multiple logistic regression was proposed to predict the direction of heat flow. Despite the effectiveness of these neural-network methods, they suffer from a fundamental drawback, namely the lack of physical transparency of the calculations.

In the present study, a different approach is proposed. It is based on predicting air microclimate parameters at the junctions of downcast shafts with underground levels using a convective-diffusive heat and mass transfer model that accounts for processes occurring in the shaft atmosphere, the shaft lining, and the surrounding rock mass. Through physical analysis, the main dimensionless complexes of the problem are identified, and the parameters governing the attenuation of the amplitude of diurnal temperature fluctuations along the airflow path are determined.

Methodology. Experimental Measurements

To investigate the thermal damping effect, a series of *in situ* experiments was carried out under the conditions of potash mines. The objects of study were a downcast shaft of a mine developing the Verkhnekamskoye potash-magnesium salt deposit (shaft N 1) and a downcast shaft of a mine developing the Gremyachinskoye potash salt deposit (shaft N 2). Both mines employ a central ventilation scheme, in which fresh air is supplied to the mine through downcast shafts and exhausted through upcast ventilation shafts under the action of a pressure depression created by the main surface-mounted ventilation fans. During the cold season, air-handling systems have a significant influence on the formation and maintenance of the required air temperature in downcast shafts, as they largely determine the thermal operating regime of mine shafts [33]. During the warm season, the air-handling systems are switched off.

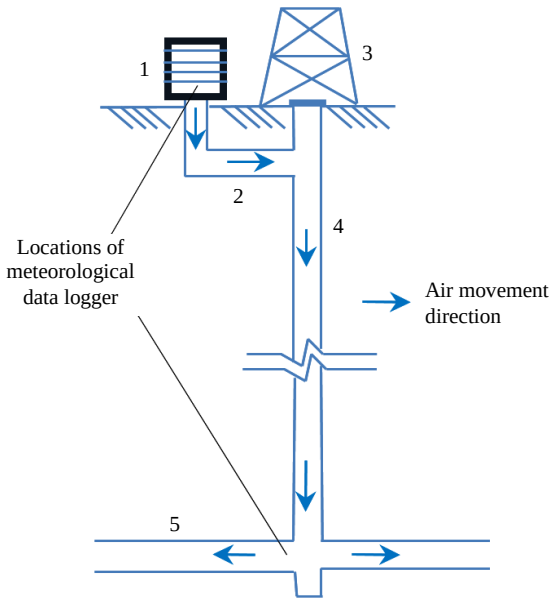


Fig.1. Layout of meteorological data logger installation in the downcast shaft

1 – the summer air intake unit of the heater installation; 2 – air supply duct; 3 – pithead building; 4 – air supply shaft; 5 – haulage level

During the *in situ* investigations conducted in the warm season, diurnal variations in the temperature and humidity of the air supplied to the mine through the downcast shafts were measured. For this purpose, portable meteorological data loggers Kestrel Drop D3 were installed at the summer air intake of the downcast shaft and in the underground section at the junction of the downcast shaft with the haulage level. These devices recorded temperature and relative humidity of the incoming airflow. The data loggers are capable of long-term data storage with a user-defined sampling interval. During the measurements, temperature and relative humidity were recorded at 5-min intervals. The measurement accuracy of the data loggers is ±0.9 °C for temperature and ±2 % for relative humidity. The installation layout of the data loggers in the downcast shaft is shown in Fig.1.

This is an open access article under the CC BY 4.0 license

The air flow rate was determined based on direct measurements of airflow velocity and the cross-sectional area of the excavation in the ventilation workings of the shaft bottom chamber. Airflow velocity was measured using an APR-2 anemometer with an accuracy of ± 0.10 + 0.05V m/s, where V is the measured velocity. The cross-sectional area of the excavation was determined by direct measurements of individual cross-sectional segments followed by calculation of the total area based on the measured parameters, using a Leica Disto X3 laser distance meter with an accuracy of $\pm 2\ (1.0 + 0.1 \cdot 10^{-3} X)$ mm, where X is the measured distance.

Downcast shaft N 1 has a clear diameter of 7 m and is equipped with a combined skip-cage hoisting system. The distance from the air intake to the junction with the haulage level is 381 m. The volumetric airflow rate through the shaft reaches 9500 m^3/min, with an average airflow velocity of 4.1 m/s.

Downcast shaft N 2 has a clear diameter of 8 m and is equipped with a skip hoisting system. The depth of the junction with the haulage level is 1094 m. The volumetric airflow rate through the shaft is 19,000 m^3/min, and the average airflow velocity in the shaft is 6.3 m/s.

Both shafts are supported by cast-iron tubbing lining with tubbing back thicknesses ranging from 30 to 70 mm and a behind-tubbing concrete layer with a thickness of 600-750 mm.

Mathematical model

The process of unsteady coupled heat exchange between the airflow, shaft lining, and surrounding rock mass, including moisture transfer, is described by a system of differential equations for convective heat transfer in the shaft airspace

$$\rho_a c_v \frac{dT}{dx} = \frac{P}{\rho_a}\frac{d\rho_a}{dx} - \rho_a L \frac{dm}{dx} + \frac{4}{D}\frac{\alpha}{V}\left(T_m\left(t, D/2, x\right) - T\right) \tag{1}$$

and heat conduction in the lining and surrounding rock mass

$$\frac{\partial T_m\left(t,r,x\right)}{\partial t} = a_m \frac{1}{r}\frac{\partial}{\partial r}\left(r\frac{\partial T_m\left(t,r,x\right)}{\partial r}\right). \tag{2}$$

The model (1) incorporates state equations for moist air:

$$\rho_a = \frac{29P - 0.11\varphi\left[479 + \left(11.52 + 1.62T\right)^2\right]}{8.314\left(T + 273\right)}; \tag{3}$$

$$\varphi = \frac{Pm}{611\left(0.622 + m\right)\exp\left(\dfrac{17.5T}{T + 241.5}\right)}; \tag{4}$$

$$P = P_0 + \rho_0 g x. \tag{5}$$

The boundary condition for the air temperature at the shaft inlet is specified based on experimental measurements:

$$T\left(t,0\right) = T_0\left(t\right). \tag{6}$$

At the initial time, the temperature of the surrounding rock mass at depth x is assumed to be uniform along the radial coordinate r:

$$T_m\left(0,r,x\right) = T_{m0}\left(x\right). \tag{7}$$

The boundary conditions for equation (2) far from the shaft contour correspond to the temperature of the undisturbed rock mass at the given depth:

$$T_m\left(t, R_{out}, x\right) = T_{m0}\left(x\right). \tag{8}$$

This is an open access article under the CC BY 4.0 license

Journal of Mining Institute. 2026. Vol. 277. P. 94-106
© Mikhail A. Semin, Evgenii V. Kolesov, Ruslan R. Gazizullin, Stanislav V. Maltsev, 2026

The outer radius of the thermal influence zone of the excavation can be estimated from equation (8) according to [34]:

$$R_{out} = \sqrt{4a_m \tau Ln\left(\frac{s\Delta T_0}{4\pi a_m \tau \delta}\right)}. \quad (9)$$

At the shaft contour, the boundary condition for equation (2) is specified in accordance with the Newton – Richman law:

$$\lambda \frac{\partial T_m}{\partial r}\bigg|_{r\to D/2} = \alpha\left(T - T_m\right)\big|_{r\to D/2}. \quad (10)$$

The effective heat-transfer coefficient between the airflow and the shaft lining is determined as follows [11]:

$$\alpha = k \cdot 3.6 \frac{V^{0.8}}{D^{0.2}}. \quad (11)$$

In the system of equations (1)-(11), the following notations are used: ρ_a is the air density in the shaft, kg/m^3; c_v is the specific isochoric heat capacity of air, J/(kg·°C); T is the air temperature in the shaft, °C; P is the barometric air pressure at depth x, Pa; L is the latent heat of water condensation, J/kg; m is the air moisture content, specified in the model based on experimental measurements, kg/kg; D is the shaft diameter, m; V is the airflow velocity in the shaft, m/s; s is the heat-exchange surface area, m^2; τ is the total duration of the heat-exchange process, s; ΔT_0 is the initial temperature mismatch between the airflow and the shaft lining, °C; δ is the temperature perturbation at the boundary of the thermal equalization layer, taken as 0.1 °C; α is the effective heat-transfer coefficient, W/(m^2·°C); k is the dimensionless empirical coefficient accounting for wall roughness and moisture content; $T_m(t, r, x)$ is the shaft wall temperature, °C; a_m is the effective thermal diffusivity of the "shaft lining – rock mass" system, m^2/s [35].

Let us introduce the dimensionless variables in the following form:

$$\hat{x} = \frac{x}{H}; \quad \hat{T} = \frac{T}{\Delta T_A}; \quad \hat{P} = \frac{P}{P_0}; \quad \hat{T}_m = \frac{T_m}{\Delta T_A}; \quad \hat{t} = \frac{t}{\Delta t_{day}}; \quad \hat{\rho} = \frac{\rho}{\rho_0}; \quad \hat{r} = \frac{r}{D},$$

where H is the shaft depth, m; ΔT_A is the surface atmospheric air temperature difference, °C; Δt_{day} = = 24 h = 86400 s is the period of atmospheric air temperature variation.

Equations (1) and (2) are reduced to the dimensionless form:

$$\hat{\rho}\frac{\partial \hat{T}}{\partial \hat{x}} = K_c \frac{\hat{P}}{\hat{\rho}}\frac{\partial \hat{\rho}}{\partial \hat{x}} - \frac{1}{Ste}\hat{\rho}\frac{\partial m}{\partial \hat{x}} + K_h\left(\hat{T}_m - \hat{T}\right);$$

$$\frac{\partial \hat{T}_m}{\partial \hat{t}} = Fo\frac{1}{\hat{r}}\frac{\partial}{\partial \hat{r}}\left(\hat{r}\frac{\partial \hat{T}_m}{\partial \hat{r}}\right);$$

the boundary condition (10) in dimensionless form takes the following form:

$$\frac{\partial \hat{T}_m}{\partial \hat{t}}\bigg| = Bi\left(\hat{T} - \hat{T}_m\right)\big|_{\hat{r}\to 1/2};$$

$$Bi = \frac{\alpha D}{\lambda}, \quad Fo = \frac{a_m \Delta t_{day}}{D^2}; \quad Ste = \frac{c_v \Delta T_A}{L}; \quad K_c = \frac{P_0}{\rho_0 c_v \Delta T_A}; \quad K_h = \frac{4\alpha H}{\rho_0 c_v D V},$$

where Bi, Fo, and Ste are dimensionless complexes representing the Biot, Fourier, and Stefan similarity numbers, respectively; K_c and K_h are additional dimensionless complexes.

This is an open access article under the CC BY 4.0 license

When the surrounding rock mass is modeled as a multilayer structure "tubbing – concrete lining – rock mass", additional dimensionless complexes appear in the model, representing the ratios of thermal diffusivities of the individual layers.

The Biot number characterizes the ratio of heat transfer within the rock mass to heat transfer at the air-wall boundary. The Fourier number describes the relationship between the rate of change of thermal conditions in the surrounding air and the rate of temperature field adjustment within the "lining – rock mass" system. The Stefan number is defined as the ratio of the characteristic change in the sensible heat of the airflow to the change in latent heat due to moisture phase transitions in the airflow. The dimensionless numbers K_c and K_h characterize, respectively, the intensity of air heating due to its downward movement along the shaft and due to its interaction with the shaft walls.

Results and discussion

As a result of the experimental campaign, time histories of air temperature and relative humidity were obtained at the mine surface, as well as at the junctions of downcast shafts with the haulage levels. The measurement results for shaft N 1 are shown in Fig.2; the monitoring duration was 78 h. From Fig.2, *a* it can be seen that, at the depth of the haulage level, a phase shift of the diurnal temperature oscillations occurs (daily lag) relative to the temperature variations observed at the mine surface. The phase lag ranges from 20 to 65 min. During the investigated period, the average amplitude of diurnal temperature variations at the surface was 5.8 °C, whereas at the underground level it decreased to 2.6 °C. This indicates a pronounced manifestation of the thermal damping effect. The air humidity also exhibits diurnal fluctuations (Fig.2, *b*). The average variation of relative humidity of atmospheric air during the observation period reached 23 % at the surface, while at the haulage level the average variation was 17 %. This confirms that, as the airflow moves down the downcast shaft, not only temperature oscillations but also relative humidity oscillations are substantially attenuated.

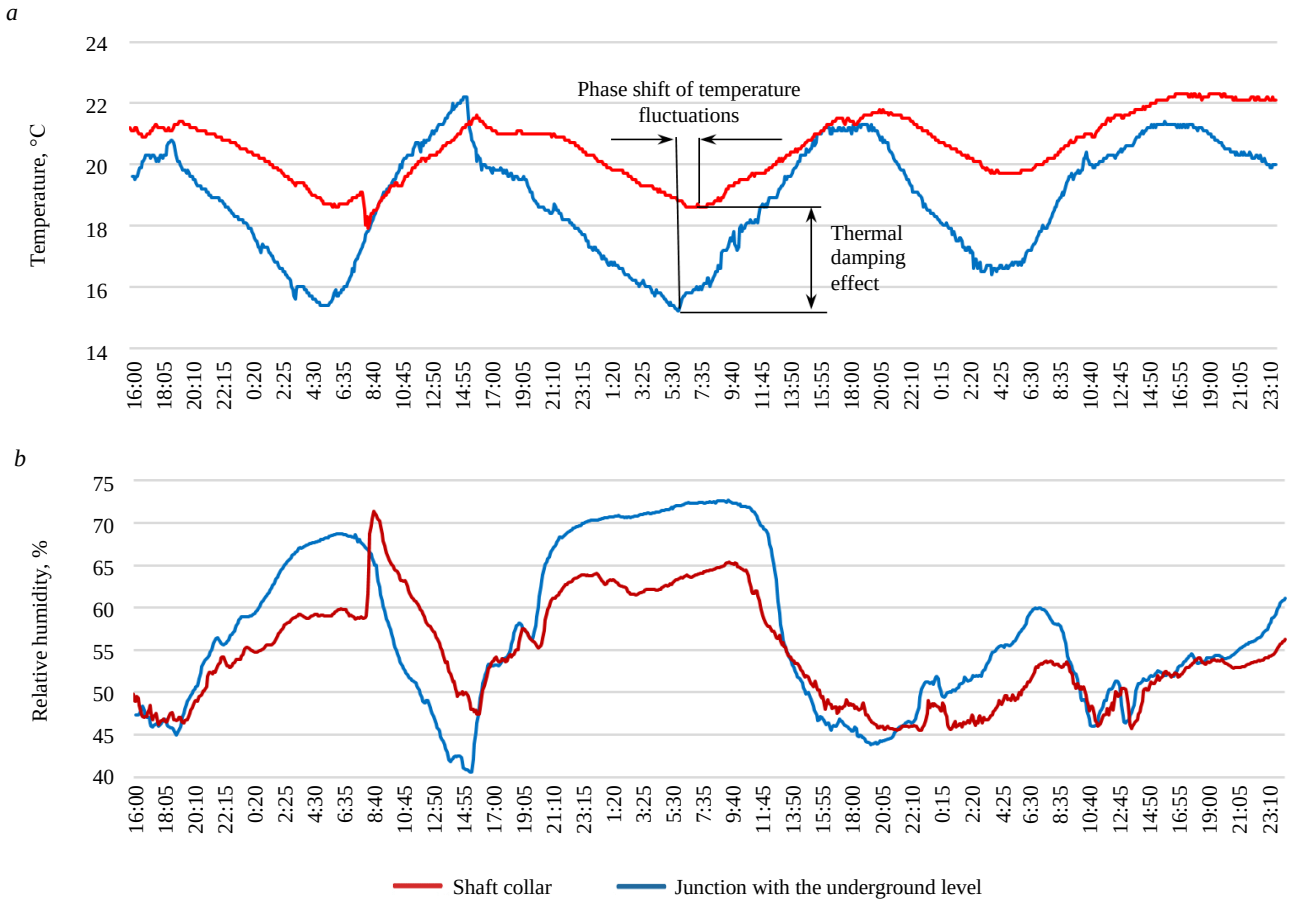


Fig.2. Diurnal variations in air temperature (*a*) and relative humidity (*b*) in shaft N1

This is an open access article under the CC BY 4.0 license

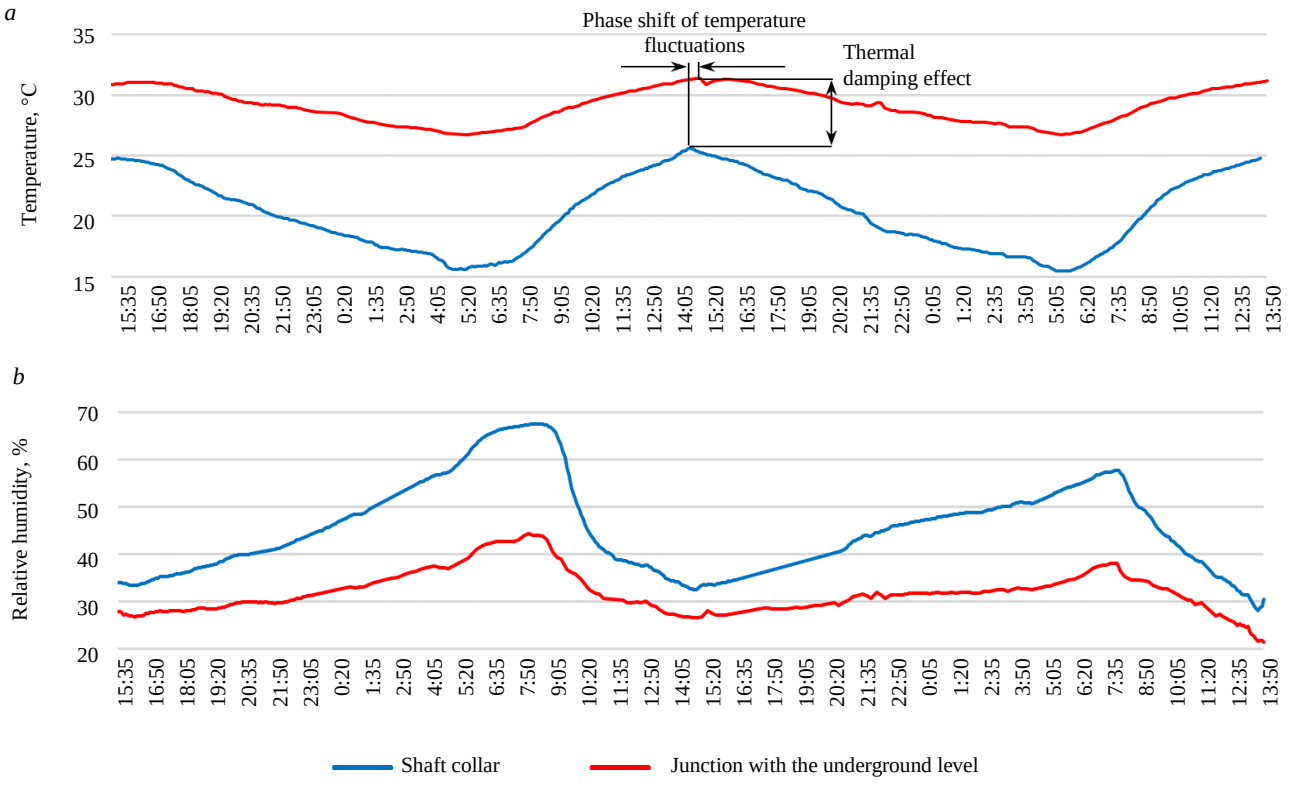


Fig.3. Diurnal variations in air temperature (*a*) and relative humidity (*b*) in shaft N 2

For shaft N 2, measurements were carried out over a period of 46 h. Figure 3, *a* shows a phase shift of diurnal temperature oscillations at the depth of the haulage level of 10-15 min relative to the surface temperature variations. Over this time interval, the air mass passing through the shaft cooled from 31.3 to 25.6 °C during daytime conditions. During nighttime (cold) periods, over the same time interval, the air temperature decreased from 26.7 to 15.6 °C while flowing down the shaft. The average amplitude of diurnal atmospheric air temperature variations was 9.7 °C, whereas the corresponding value at the junction with the underground level was 4.5 °C, which again reflects the effect of thermal damping.

The average variation of relative humidity during the investigated period reached 32 % at the mine surface and 17 % at the haulage level, further confirming the smoothing of relative humidity oscillations of the airflow as it travels along the downcast shaft.

Substituting characteristic values typical for the investigated mine shafts yields the following orders of magnitude for the similarity numbers: Bi ~10^1-10^2; Fo ~10^{-3}-10^{-2}; Ste ~10^{-3}; K_c ~10^1; K_h ~10^0. The obtained values of the Biot and Fourier numbers indicate that the main temperature variations occur in the vicinity of the shaft surface, while temperature changes inside the rock mass are relatively small, since heat transfer into the concrete lining proceeds slowly. The small values of the Stefan number imply that significantly more heat is required for phase transitions (condensation or evaporation of moisture in the airflow) than for changing the air temperature. The orders of magnitude of K_c and K_h indicate a substantial contribution to air heating from both air compression during downward movement along the shaft and heat exchange with the shaft walls.

To preliminarily assess the contribution of each heat and mass transfer processes included in equation (1) to the increase in air temperature at the junction with the underground level, characteristic parameter values were substituted (Table 2). The average barometric pressure, average temperature, and average air density in the shafts were taken as the arithmetic mean of the corresponding parameters measured at the shaft collar and at the junction with the underground level.

This is an open access article under the CC BY 4.0 license

Table 2

Air properties and shaft parameters

Parameter	Shaft N 1	Shaft N 2
Average air density in the shaft, kg/m^3	1.235	1.26
Average barometric air pressure in the shaft, Pa	103,570	107,593
Average increase in air temperature in the shaft, °C	1.6	9.0
Average increase in moisture content in the shaft, kg/kg	0.83	0.41
Average lining temperature, °C	20.1	27.3
Shaft depth, m	381	1094
Shaft diameter, m	7	8
Air velocity in the shaft, m/s	4.1	6.3
Specific heat capacity of air, J/(kg·°C)	1005	1005
Latent heat of water condensation, kJ/kg	2260	2260
Heat-transfer coefficient between airflow and shaft wall, W/(m^2·°C)	16.6	13.5

Table 3 presents the relative contributions of various heat and mass transfer processes I_i occurring in the investigated shafts to the formation of the final air temperature at the junction with the underground level. The contribution was calculated as the ratio of the heat added to or removed from the airflow by a given factor to the change in internal energy of the airflow:

$$I_i = \frac{W_i}{\rho_a c_a \Delta T} \cdot 100\ \%,$$

where W_i is the heat associated with the i-th thermal factor.

The total contribution of all heat and mass transfer processes for each shaft equals 100 %, meaning that the entire change in air temperature within the shaft is explained by these processes.

Table 3

Relative contribution of heat and mass transfer processes to air temperature at the shaft-underground level junction, %

Factor	Shaft N 1	Shaft N 2
Hydrostatic air heating due to compression	+196.9	+84.8
Moisture evaporation from the shaft surface	–116.6	–10.2
Heat exchange with the shaft lining	+19.7	+25.4

Note. A positive sign indicates that the factor contributes to an increase in air temperature with depth, while a negative sign indicates cooling.

Table 3 shows that, for shaft N 1, the dominant factor contributing to air temperature increase is hydrostatic heating due to adiabatic compression, which is approximately ten times greater than the contribution from heat exchange with the shaft lining. At the same time, a significant portion of the airflow energy is expended on moisture evaporation from the lining surface. For shaft N 2, hydrostatic heating due to adiabatic compression also dominates over heat exchange with the lining (by a factor of 3.3); however, owing to the lower moisture content, energy losses due to evaporation are relatively small.

The system of equations (1)-(11) was solved using the finite difference method, employing a first-order explicit time scheme and a second-order central spatial scheme. As a result, time-dependent air temperature profiles at the shaft bottom near the underground level were obtained. The parameters a_m and k were treated as adjustable and were determined by successive approximations so that the results of the modeled air temperature $\tilde{T}(t_i)$ matched the experimental measurements as closely as possible, i.e., satisfying condition

This is an open access article under the CC BY 4.0 license

$$\sqrt{\frac{\sum_{i=1}^{n}\left(\tilde{T}(t_i)-T(t_i)\right)^2}{n}} \to \min. \qquad (12)$$

Figure 4 shows contour lines of the root mean square error (12) in the phase plane "coefficient k – thermal diffusivity of the rock mass" for the conditions of shaft N 2. The minimum of functional (12) is achieved at $k = 1.3$ and an effective rock-mass thermal diffusivity $a_m = 2.2 \cdot 10^{-7}$ m^2/s. Figure 5 presents the time evolution of air temperature at the surface and at the junction with the underground level. Curve 3 in Fig.5 corresponds to the solution of equations (1)-(11) obtained with $k = 1.3$ and $a_m = 2.2 \cdot 10^{-7}$ m^2/s.

Figure 6 shows contour lines of the root mean square error (12) in the "coefficient k – thermal diffusivity of the rock mass" phase plane for shaft N 1. The minimum of functional (12) is reached at $k = 2.2$ and an effective thermal diffusivity $a_m = 150 \cdot 10^{-7}$ m^2/s. Figure 7 presents the time evolution of air temperature at the surface and at the junction with the underground level. Curve 3 in Fig.7 was obtained by solving equations (1)-(11) with $k = 2.2$ and $a_m = 150 \cdot 10^{-7}$ m^2/s.

Thus, the mathematical model of unsteady conjugate heat transfer between the airflow, shaft lining, and surrounding rock mass, including moisture transport and calibrated using experimental data, can be applied to predict the temporal evolution of air temperature at the underground level with accuracy sufficient for engineering calculations. The minor deviations between modeled curves and experimental data are mainly attributable to instrumental measurement errors.

The calibrated models for both shafts were subsequently used to determine the functional dependence of the underground level air temperature $T_{\text{lev}}(t)$ on the surface air temperature $T_{\text{A}}(t)$ and shaft depth H. For this purpose, a harmonic variation of surface temperature was specified as boundary condition (6):

$$T_{\text{A}}(t) = \bar{T}_{\text{A}} + \frac{\Delta T_{\text{A}}}{2}\cos\left(\frac{2\pi t}{1440}\right),$$

where $\bar{T}_{\text{A}}$ is the daily mean surface temperature, °C; ΔT_{A} is the amplitude of diurnal atmospheric air temperature variations, °C; t is time, min. The parameters $\bar{T}_{\text{A}}$, ΔT_{A}, and H were varied.

The results of multiparametric modeling made it possible to establish the dependence of underground air temperature on the varied parameters. The dependencies were approximated as a superposition of a time-averaged air temperature and an unsteady component representing harmonic oscillations about this mean value, with certain phase shifts caused by the inertia of the heat conduction process. As a result of the multiparametric simulations, the following expressions were obtained for predicting air temperature at the underground level for the investigated shafts:

$$T_{\text{lev}}(t)_2 = \bar{T}_{\text{A}} + 0.0073H + \frac{18.3\Delta T_{\text{A}}}{H^{0.6}}\cos\left(0.048 + \frac{2\pi t}{1440}\right);$$

$$T_{\text{lev}}(t)_1 = \bar{T}_{\text{A}} + 0.0056H + \frac{9.3\Delta T_{\text{A}}}{H^{0.6}}\cos\left(0.109 + \frac{2\pi t}{1440}\right).$$

The second terms in these expressions characterize the effect of the temperature gradient resulting from the combined influence of hydrostatic compression and the time-averaged heat exchange with the surrounding rock mass.

This is an open access article under the CC BY 4.0 license

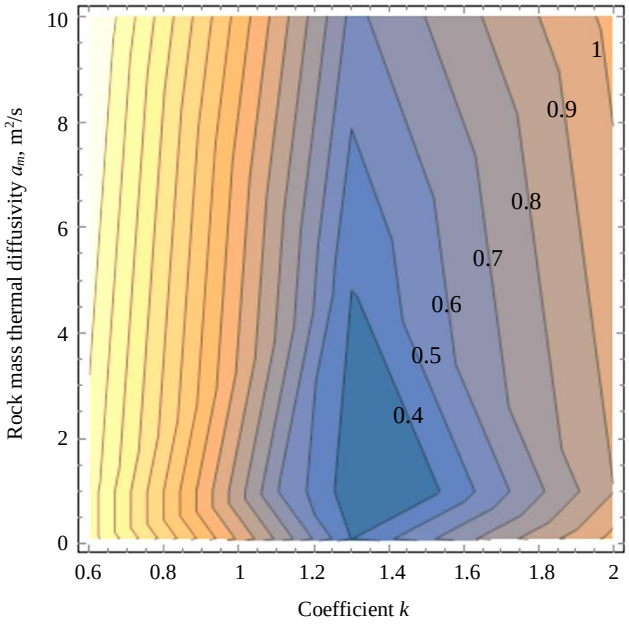


Fig.4. Contour lines of the root mean square error (12) in the phase plane "coefficient k – rock mass thermal diffusivity a_m" for shaft N 2

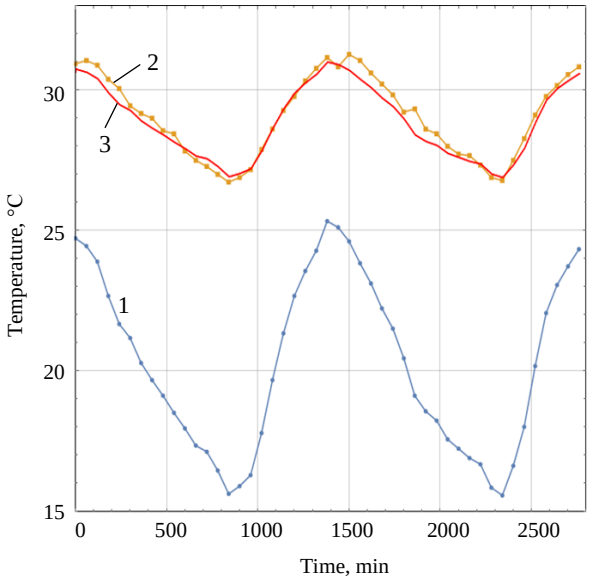


Fig.5. Temporal dynamics of air temperature in shaft N 2
1 – *in situ* measurements at the shaft collar;
2 – *in situ* measurements at the junction of the shaft with the underground level; 3 – calculated temperature dynamics at the junction of the shaft with the underground level

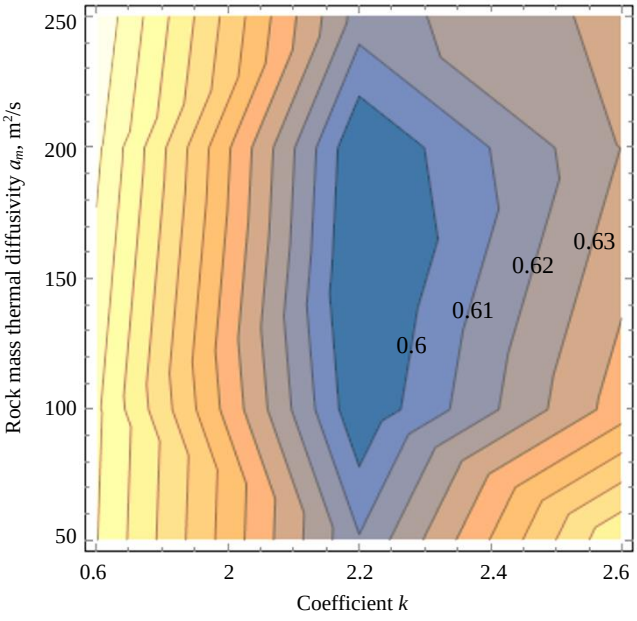


Fig.6. Contour lines of the root mean square error (12) in the phase plane "coefficient k – rock mass thermal diffusivity a_m" for shaft N 1

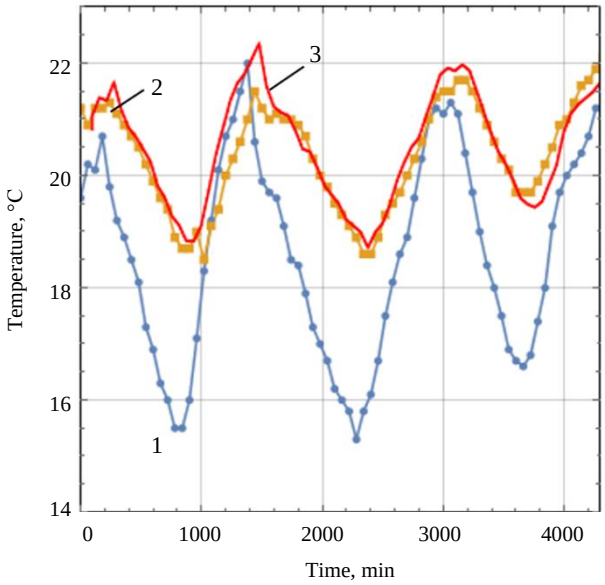


Fig.7. Temporal dynamics of air temperature in shaft N 1
1 – *in situ* measurements at the shaft collar;
2 – *in situ* measurements at the junction of the shaft with the underground level; 3 – modelled temperature dynamics at the junction of the shaft with the underground level

The general form of the calculation formulas for determining the mean air temperature in the shaft bottom chamber of a downcast shaft $\overline{T}_{\text{lev}}$, the diurnal temperature variation ΔT_{lev} and the phase shift of temperature oscillations φ is given by:

$$\overline{T}_{\text{lev}} = \overline{T}_{\text{A}} + aH;$$

This is an open access article under the CC BY 4.0 license

© Mikhail A. Semin, Evgenii V. Kolesov, Ruslan R. Gazizullin, Stanislav V. Maltsev, 2026

$$\Delta T_{\text{lev}} = b\frac{\Delta T_{\text{A}}}{H^{0.6}};$$

$$\varphi = 2\pi\frac{\Delta t}{1440},$$

where Δt is the daily lag of temperature oscillations at the junction with the underground level relative to surface temperature oscillations, min; a and b are empirical coefficients that, in the general case, depend on the similarity numbers Bi, Fo, Ste, as well as on K_c and K_h.

Conclusion

The results of a study on the damping effect of the amplitude of diurnal variations in atmospheric air temperature and humidity in downcast shafts of potash mines are presented. The study is based on a combined theoretical and experimental approach, which includes *in situ* measurements of air microclimate parameters under underground mining conditions, as well as the application of a mathematical model of conjugate convective-diffusive heat and mass transfer within the shaft, its lining, and the surrounding rock mass, to predict air temperature at the junction of the shaft with the underground level.

A methodology for conducting in situ measurements under mine conditions is described, and the obtained data for two downcast shafts of potash mines with different depths are presented. These data were subsequently used for the parameterization and validation of the proposed model of unsteady conjugate heat transfer between the airflow, the shaft lining, and the surrounding rock mass.

Effective heat-transfer coefficients α between the airflow and the shaft wall were determined for the investigated shafts, along with the effective thermal diffusivities of the surrounding rock masses a_m. For shaft N 2, the following values were obtained $\alpha = 4.68(V^{0.8}/D^{0.2})$ W/(m$^2\cdot$°C), $a_m = 2.2\cdot10^{-7}$ m^2/s; for shaft N 1: $\alpha = 7.92(V^{0.8}/D^{0.2})$ W/(m$^2\cdot$°C), $a_m = 150\cdot10^{-7}$ m^2/s.

The calibrated models for both shafts were further employed in multiparametric simulations aimed at determining an empirical relationship for the air temperature in the shaft bottom chamber of the underground level as a function of the daily mean surface temperature, the amplitude of surface temperature oscillations, and the shaft depth. As a result, calculation formulas were derived for estimating the mean air temperature in the shaft bottom chamber of a downcast shaft, the diurnal temperature variation, and the phase shift of temperature oscillations. It is shown that the amplitude of air temperature oscillations in the shaft bottom chamber depends on its depth according to a power-law relationship with an exponent of −0.6.

The results of this study can be used for the quantitative assessment of microclimatic conditions in mine ventilation networks and for making decisions on the necessity of air-cooling systems to ensure acceptable working conditions in mines. The proposed approach to evaluating the diurnal variation of air temperature at the underground level also enables refinement of the calculation of the temporal dynamics of natural ventilation pressure, both under normal and reversed ventilation modes, which, in turn, improves the accuracy of predicting emergency ventilation scenarios in mines.

REFERENCES

1. Galkin A.F. The thermal condition of the mines in cryolite zone. *Journal of Mining Institute.* 2016. Vol. 219, p. 377-381 (in Russian). DOI: 10.18454/PMI.2016.3.377

2. Zaitsev A.V., Semin M.A., Parshakov O.S. Features of the thermal regime formation in the downcast shafts in the cold period of the year. *Journal of Mining Institute.* 2021. Vol. 250, p. 562-568. DOI: 10.31897/PMI.2021.4.9

3. Habibi A., Kramer R.B., Gillies A.D.S. Investigating the effects of heat changes in an underground mine. *Applied Thermal Engineering*. 2015. Vol. 90, p. 1164-1171. DOI: 10.1016/j.applthermaleng.2014.12.066

4. Hongbin Zhao, Shihao Tu, Xun Liu et al. Study of energy-efficient heat resistance and cooling technology for high temperature working face with multiple heat sources in deep mine. *International Journal of Coal Science & Technology*. 2023. Vol. 10. N 35. DOI: 10.1007/s40789-023-00590-9

This is an open access article under the CC BY 4.0 license

5. Fair R., van Laar J.H., Nell K. et al. Simulating the sensitivity of underground ventilation networks to fluctuating ambient conditions. *South African Journal of Industrial Engineering*. 2021. Vol. 32. N 3, p. 42-51. DOI: 10.7166/32-3-2616

6. Zaitsev A.V., Levin L.Yu., Parshakov O.S. Features of ventilation and air conditioning design in deep mines. *Gornyi zhurnal.* 2023. N 11, p. 57-63 (in Russian). DOI: 10.17580/gzh.2023.11.09

7. Levin L.Yu., Zaitsev A.V. Simulation, Design, and Control of the Thermal Regime of Deep Mines. *Doklady Earth Sciences.* 2022. Vol. 507. Part 2, p. 1160-1168. DOI: 10.1134/S1028334X22600888

8. Alabyev V.R., Novikov V.V., Pashinyan L.A., Bazhina T.P. Normalization of thermal mode of extended blind workings operating at high temperatures based on mobile mine air conditioners. *Journal of Mining Institute.* 2019. Vol. 237, p. 251-258. DOI: 10.31897/PMI.2019.3.251

9. Maurya T., Karena K., Vardhan H. et al. Potential Sources of Heat in Underground Mines – A Review. *Procedia Earth and Planetary Science.* 2015. Vol. 11, p. 463-468. DOI: 10.1016/j.proeps.2015.06.046

10. Zaitsev A., Shalimov A., Borodavkin D. Unsteady Coupled Heat Transfer in the Air and Surrounding Rock Mass for Mine Excavations with Distributed Heat Sources. *Fluids*. 2023. Vol. 8. Iss. 2. N 67. DOI: 10.3390/fluids8020067

11. Kolesov E.V., Semin M.A., Kazakov B.P., Knjazev N.A. Improvement of calculation method for heat transfer coefficient in air shaft based on experimental measurements in reversal ventilation mode. *Mining Informational and Analytical Bulletin.* 2023. N 3, p. 57-71 (in Russian). DOI: 10.25018/0236_1493_2023_3_0_57

12. Scalise K.A., Teixeira M.B., Kocsis K.C. Managing Heat in Underground Mines: the Importance of Incorporating the Thermal Flywheel Effect into Climatic Modeling. *Mining, Metallurgy & Exploration*. 2021. Vol. 38. Iss. 1, p. 575-579. DOI: 10.1007/s42461-020-00323-5

13. Tu Q., Yu C., Li Z. et al. Computer simulation study on heat transfer of surrounding rock in mine roadway of coal mine enterprises. *Thermal Science*. 2020. Vol. 24. Iss. 5. Part B, p. 3049-3058. DOI: 10.2298/TSCI191020079T

14. Pandey A., Sridharan S.J., Sastry B.S. A transient model for predicting psychrometric properties of air at an intake shaft bottom of shallow depth working. *Arabian Journal of Geosciences*. 2022. Vol. 15. Iss. 16. N 1396. DOI: 10.1007/s12517-022-10679-1

15. Duganov G.V., Baratov E.I. Thermal regime of mines. Moscow: Gosgortekhizdat, 1963, p. 144 (in Russian).

16. Stroh R.M. A Note on the Downcast Shaft as a Thermal Flywheel. *Journal of the Mine Ventilation Society of South Africa*. 1979. Vol. 32, p. 77-80.

17. Roghanchi P., Kocsis K.C. Quantifying the thermal damping effect in underground vertical shafts using the nonlinear auto-regressive with external input (NARX) algorithm. *International Journal of Mining Science and Technology*. 2019. Vol. 29. Iss. 2. P. 255-262. DOI: 10.1016/j.ijmst.2018.06.002

18. Kobylkin S.S. Systems designing of ventilation of mine. *Mining Informational and Analytical Bulletin*. 2015. N S1, p. 150-156 (in Russian).

19. Tingting Sun, Zhiwen Luo, Tim Chay. An analytical model to predict the temperature in subway-tunnels by coupling thermal mass and ventilation. *Journal of Building Engineering*. 2021. Vol. 44. N 102564. DOI: 10.1016/j.jobe.2021.102564

20. Liskova M.Yu., Vishnevskaya N.L., Plakhova L.V. Effect of microclimate on personnel in deep-level excavations of potash mines. *Mining Informational and Analytical Bulletin.* 2019. N 9, p. 219-230 (in Russian). DOI: 10.25018/0236-1493-2019-09-0-219-230

21. Vishnevskaya N.L., Liskova M.Yu., Plakhova L.V. Personnel physiology and hygiene, and occupational health and safety maintenance in deep mines: Problems and solutions. *Mining Informational and Analytical Bulletin*. 2020. N 10, p. 163-176 (in Russian). DOI: 10.25018/0236-1493-2020-10-0-163-176

22. Shuai Zhu, Jianwei Cheng, Zui Wang, Borowski M. Physical simulation experiment of factors affecting temperature field of heat adjustment circle in rock surrounding mine roadway. *Energy Sources, Part A: Recovery, Utilization, and Environmental Effects*. 2023. Vol. 45. Iss. 4, p. 11278-11295. DOI: 10.1080/15567036.2020.1760969

23. Menglong Bian, Wencai Wang. Prediction model of vertical shaft air temperature and its application. *IOP Conference Series: Earth and Environmental Science*. 2019. Vol. 384. N 012016. DOI: 10.1088/1755-1315/384/1/012016

24. Verbeke S., Audenaert A. Thermal inertia in buildings: A review of impacts across climate and building use. *Renewable and Sustainable Energy Reviews*. 2018. Vol. 82. Part 3, p. 2300-2318. DOI: 10.1016/j.rser.2017.08.083

25. Heier J., Bales C., Martin V. Combining thermal energy storage with buildings – a review. *Renewable and Sustainable Energy Reviews*. 2015. Vol. 42, p. 1305-1325. DOI: 10.1016/j.rser.2014.11.031

26. Borodavkin D.A. Calculation and Management of the Unsteady Thermal Regime in Working Areas of Long Extraction Faces (Case Study: Starobinskoye Potash Deposit): Avtoref. dis. … kand. tekhn. nauk. Perm: Mining Institute of the Ural Branch of the Russian Academy of Sciences, 2024, p. 23 (in Russian).

27. Rudakov M.L., Stepanov I.S. Assessment of professional risk caused by heating microclimate in the process of underground mining. *Journal of Mining Institute.* 2017. Vol. 225, p. 364-368. DOI: 10.18454/PMI.2017.3.364

28. Parshakov O.S. Results of the Study of the Mine Ventilation Network of the Norilsk Industrial District. *Gornoe ekho*. 2021. N 4 (85), p. 119-128. DOI: 10.7242/echo.2021.4.23

29. Semin M., Levin L. Mathematical Modeling of Air Distribution in Mines Considering Different Ventilation Modes. *Mathematics*. 2023. Vol. 11. Iss. 4. N 989. DOI: 10.3390/math11040989

30. Stewart C., Aminossadati S.M., Kizil M.S., Andreatidis T. Diurnal Thermal Flywheel Influence on Ventilation Temperatures in Large Underground Mines. Proceedings of the 16th North American Mine Ventilation Symposium, 17-22 June 2017, Golden, CO, USA. Colorado School of Mines, 2017, p. 9-1 – 9-8.

31. Pandey A., Mondal C., Sastry B.S. Multiple logistic regression based prediction of heat flow direction in an intake incline of shallow depth by integrating thermal flywheel effect: A case study. *Applied Thermal Engineering*. 2022. Vol. 213. N 118765. DOI: 10.1016/j.applthermaleng.2022.118765

This is an open access article under the CC BY 4.0 license

32. Scalise K.A., Kocsis K. Utilizing Nonlinear Autoregressive with Exogenous Input Neural Networks to Evaluate the Thermal Flywheel Effect Along Intake Shafts at Nevada Mines. *Mining, Metallurgy & Exploration*. 2021. Vol. 38. Iss. 3, p. 1395-1410. DOI: 10.1007/s42461-021-00411-0

33. Anderson R., De Souza E. Heat stress management in underground mines. *International Journal of Mining Science and Technology*. 2017. Vol. 27. Iss. 4, p. 651-655. DOI: 10.1016/j.ijmst.2017.05.020

34. Zaitsev A.V. Development of Methods for Normalizing Microclimatic Conditions in Underground Workings of Deep Mines: Avtoref. dis. … kand. tekhn. nauk. Perm: Mining Institute of the Ural Branch of the Russian Academy of Sciences, 2013, p. 20 (in Russian).

35. Kolesov E.V. Development of Methods for Controlling Drip Moisture in Mine Ventilation Shafts: Avtoref. dis. … kand. tekhn. nauk. Perm: Mining Institute of the Ural Branch of the RAS, 2023, p. 24 (in Russian).

***Authors*: Mikhail A. Semin,** *Doctor of Engineering Sciences, Head of Laboratory* (*Mining Institute of the Ural Branch of the RAS, Perm, Russia*), *https://orcid.org/0000-0001-5200-7931*, **Evgenii V. Kolesov,** *Candidate of Engineering Sciences, Researcher* (*Mining Institute of the Ural Branch of the RAS, Perm, Russia*), *kolesovev@gmail.com, https://orcid.org/0000-0002-0755-7405*, **Ruslan R. Gazizullin,** *Leading Engineer (Mining Institute of the Ural Branch of the RAS, Perm, Russia*), *https://orcid.org/0009-0004-3122-1647*, **Stanislav V. Maltsev,** *Candidate of Engineering Sciences, Head of Sector* (*Mining Institute of the Ural Branch of the RAS, Perm, Russia*), *https://orcid.org/0009-0002-9887-1455*.

The authors declare no conflict of interests.

This is an open access article under the CC BY 4.0 license